

Lithium and sodium in the globular cluster M 4

Detection of a Li-rich dwarf star: preservation or pollution?*

L. Monaco¹, S. Villanova², P. Bonifacio³, E. Caffau^{4,3**}, D. Geisler², G. Marconi¹, Y. Momany¹ and H.-G. Ludwig^{4,3}

¹ European Southern Observatory, Casilla 19001, Santiago, Chile

² Universidad de Concepción, Casilla 160-C, Concepción, Chile

³ GEPI, Observatoire de Paris, CNRS, Univ. Paris Diderot ; Place Jules Janssen, 92190 Meudon, France

⁴ Zentrum für Astronomie der Universität Heidelberg, Landessternwarte, Königstuhl 12, 69117 Heidelberg, Germany

Received; accepted

ABSTRACT

Context. The abundance inhomogeneities of light elements observed in Globular Clusters (GCs), and notably the ubiquitous Na-O anti-correlation, are generally interpreted as evidence that GCs comprise several generations of stars. There is an on-going debate as to the nature of the stars which produce the inhomogeneous elements, and investigating the behavior of several elements is a way to shed new light on this problem.

Aims. We aim at investigating the Li and Na content of the GC M 4, that is known to have a well defined Na-O anti-correlation.

Methods. We obtained moderate resolution ($R=17\,000-18\,700$) spectra for 91 main sequence (MS)/sub-giant branch stars of M 4 with the Giraffe spectrograph at the FLAMES/VLT ESO facility. Using model atmospheres analysis we measured lithium and sodium abundances.

Results. We detect a weak Li-Na anti-correlation among un-evolved MS stars. One star in the sample, # 37934, shows the remarkably high lithium abundance $A(\text{Li})=2.87$, compatible with current estimates of the primordial lithium abundance.

Conclusions. The shallow slope found for the Li-Na anti-correlation suggests that lithium is produced in parallel to sodium. This evidence, coupled with its sodium-rich nature, suggests that the high lithium abundance of star # 37934 may originate by pollution from a previous generations of stars. The recent detection of a Li-rich dwarf of pollution origin in the globular cluster NGC 6397 may also point in this direction. Still, no clear cut evidence is available against a possible preservation of the primordial lithium abundance for star # 37934.

Key words. nuclear reactions, nucleosynthesis, abundances, stars: abundances, stars: Population II, (Galaxy:) globular clusters: individual M 4, galaxies: abundances, cosmology: observations

1. Introduction

For many years astronomers have assumed Galactic Globular Clusters (GCs) as an example of Single Stellar Population, which constitutes the ideal test-bench for stellar evolution theories. This view came about mainly by considering the narrow Red Giant Branches (RGB) which characterize the color-magnitude diagrams (CMDs) of such systems. A theoretical isochrone of a single metallicity and age, typically fits well the observed color-magnitude diagrams. Disturbing information, such as the scatter in Na abundances in M3 and M13 noted by Cohen (1978) or the variation in CN or CH strengths (Norris, 1981; Norris & Freeman, 1983) or other chemical inhomogeneities which emerged from spectroscopic analysis, were typically blamed on mixing processes in the RGB stars. It was only when it was shown that chemical inhomogeneities persist down to Turn-Off stars (TO, Hesser, 1978; Cannon et al., 1998; Gratton et al., 2001), which in their centers have temperatures too low to allow the nuclear reactions which may give rise to the observed anomalies (e.g. the Na enrichment), that

it became necessary to accept that multiple stellar populations have contributed to the present day chemical composition of GCs. Different scenarios and possible polluters from which multiple populations in GCs may originate have been proposed and, in this respect, gathering information about different chemical species is crucial to consolidate the observational framework and constrain the models (see, e.g., Decressin et al., 2007; Ventura & D’Antona, 2010; D’Ercole et al., 2010; Valcarce & Catelan, 2011).

Further evidence on the complex nature of GCs has been accumulating in recent years. Besides the spectacular case of ω Cen (see, e.g., Villanova et al., 2007, and references therein) which is now commonly considered as the remnant nucleus of an accreted dwarf galaxy, recent high accuracy color-magnitude diagrams obtained using ACS@HST data, have revealed that several among the most massive globular clusters (NGC2808, NGC1851, NGC6388, NGC6441) present photometric evidence for multiple sequences at the main sequence (MS) and/or sub-giant branch (SGB) level (see Piotto, 2008, for a review).

Globular Clusters are among the oldest objects in the universe and, in spite of the mentioned chemical anomalies, the first generation (FG) of stars in GCs is, however, easily identified by its low Na content. It is interesting in this context that all of the GCs studied so far (ω Cen, NGC 6752, NGC 6397, 47 Tuc, M 4,

* Based on observations taken at ESO VLT Kueyen telescope (Cerro Paranal, Chile, program: 085.D-0537A).

** Gliese Fellow

Correspondence to: lmonaco@eso.org

see Monaco et al., 2010; Mucciarelli et al., 2011, and references therein), present – at least in their FG of stars – a Li content comparable to that of warm metal-poor halo dwarfs, i.e. the so-called *Spite plateau* (Spite & Spite, 1982; Sbordone et al., 2010). The simplest interpretation of the *Spite plateau* is that the lithium observed in these old stars is the lithium produced during the Big Bang (Iocco et al., 2009). If this is the case, however, there is a “cosmological lithium problem”, because the level of the *Spite plateau* is a factor of three to five lower than the primordial lithium predicted by Standard Big Bang Nucleosynthesis and the baryonic density measured from the fluctuations of the Cosmic Microwave Background (see, e.g., Monaco et al., 2010; Sbordone et al., 2010, and references therein).

In this letter, we report the results of our investigation of the lithium and sodium abundances in MS/SGB stars in the GC M 4, based on FLAMES-GIRAFFE/VLT spectra (Pasquini et al., 2002).

2. Observations and data reduction

We observed stars along the M 4 MS and SGB using the FLAMES/GIRAFFE spectrograph at ESO Paranal (open circles in the left panel of Fig.1). Observations were conducted in service mode between April and July 2010 using the HR12 and HR15N settings. The former covers the Na-D doublet at a resolution of 18 700. The HR15N setting covers the Li I resonance doublet at 670.8 nm, as well as the H α region at a resolution of 17 000. The same plate configuration was used for both settings. Each target was observed for ~ 2.3 hr and ~ 10 hr total integration time in the two settings, respectively. Frames were processed using version 2.13 of the FLAMES/GIRAFFE data reduction pipeline¹. Ninety-nine medusa fibers were allocated to M 4 stars, while 15 fibers were assigned to positions selected for sky subtraction. Sky holes were selected at similar radial distances from the clusters center as the science targets and the average of the 15 sky fibers was subtracted from the science spectra.

The standard IRAF² task *fxcor* was employed to measure the stellar radial velocities by cross-correlating the spectra with synthetic ones of similar atmospheric parameters. Corrections to the heliocentric system were computed using the IRAF task *rvcorrect* and applied to the observed radial velocities. After being reduced to rest frame, multiple spectra of the same target were finally averaged. We obtain spectra with a signal-to-noise ratio (SNR) in the range 72-152 and 19-65 at the Li resonance doublet and the Na-D doublet, respectively. A sample of the obtained spectra in the Li resonance doublet region is presented in Fig.1 (right panel).

We obtain a cluster mean radial velocity and dispersion of $v_{helio}=71.4\pm 0.4$ km s⁻¹, $\sigma=3.7\pm 0.2$ km s⁻¹, after excluding three stars, deviating more than $3\text{-}\sigma$ from the mean, and five stars presenting discordant T_{eff} as estimated from the B-V and V-I colors (see below). These values are in good agreement with the recent measures by Marino et al. (2008) and Lovisi et al. (2010).

3. Abundance analysis

The cluster photometry we adopt in this contribution is based on data collected with the Wide Field Imager (WFI) mounted

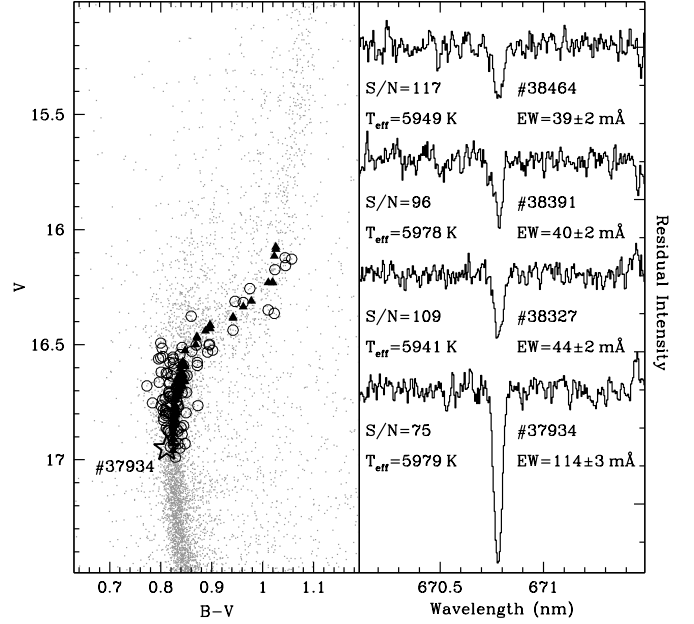


Fig. 1. Left panel: V vs B-V M 4 color-magnitude diagram. Target stars are marked by open circles. Filled triangles mark the location of the target as projected on the cluster mean ridge line. Target # 37934 is marked by the star symbol. Right panel: summed spectra for a subsample of the target stars.

at the 2.2m telescope at the La Silla observatory, which was reduced following Momany et al. (2003) and was first corrected for differential reddening following the recipe by Sarajedini et al. (2007). We derived the target stars effective temperatures (T_{eff}) from the B-V and V-I colors as projected on the mean cluster ridge line and using the Alonso et al. (1996) calibrations. We adopted for the cluster a mean reddening of $E(B-V)=0.36$ (Harris, 1996). The projection we applied is meant to provide a more robust determination of the targets colors, particularly given the presence of a significant differential reddening in the cluster. Indeed, we obtain a good agreement between the T_{eff} derived from the B-V and V-I colors and we eventually adopted their average. Five stars were excluded from the sample, because of their discrepant positions in the V vs B-V and V vs V-I CMDs, which converted in temperatures derived from the B-V and V-I colors different by more than 100 K.

We also estimated the stellar T_{eff} by fitting for each star the H α line with synthetic profiles calculated using the SYNTHE code (Sbordone et al., 2004; Sbordone, 2005; Kurucz, 2005). The two temperature scales are in excellent agreement, with a mean difference of -6 ± 5 K ($\sigma_{\Delta(T_{eff})}=60$ K). The accuracy of the T_{eff} determination using H α line fitting is usually, however, of the order of ~ 150 K and is dominated by uncertainties in the continuum normalization and/or in the correction of the blaze function of the spectrograph (Bonifacio et al., 2007; Sbordone et al., 2010; Monaco et al., 2010). In the following we will adopt 150 K as uncertainty on the T_{eff} determination.

Surface gravities were determined with the aid of theoretical isochrones and vary in the range $\log g=3.48\text{--}4.13$. In order to determine the stellar micro-turbulent velocity (ξ), stars were first grouped by T_{eff} in four sub-samples. For each sub-sample, a high SNR mean spectrum was generated averaging together all the spectra. ξ was then fixed, as usual, by minimizing the de-

¹ <http://girbltdrs.sourceforge.net/>

² IRAF is distributed by the National Optical Astronomy Observatories, which is operated by the association of Universities for Research in Astronomy, Inc., under contract with the National Science Foundation.

pendence of the derived abundances on the measured equivalent widths (EWs), for a selected sample of iron lines. The Marino et al. (2008) line-list was employed for this purpose and EWs were measured by Gaussian fitting. The derived trend of ξ as a function of T_{eff} was used to assign individual ξ values to the target stars.

We adopted the above atmospheric parameters to calculate proper ATLAS-9 model atmospheres which we used, along with the MOOG code (Snedden, 1973), to derive the Fe and Na abundances. For each star, iron abundances were measured using the two lines at 6995.0 Å and 6678.0 Å. We obtain a mean $[\text{Fe}/\text{H}] = -1.31 \pm 0.03$ dex (Gaussian dispersion for 71 stars) for MS stars at $T_{\text{eff}} > 5880$ K. This value raises to $[\text{Fe}/\text{H}] = -1.17 \pm 0.03$ dex for the 10 brighter/cooler stars in our sample ($T_{\text{eff}} < 5600$ K). This latter value is in fair agreement (within 0.1 dex) with previous estimates for RGB/SGB stars (Ivans et al., 1999; Marino et al., 2008; Carretta et al., 2009; Mucciarelli et al., 2011). Although compatible within the errors (≈ 0.10 - 0.15 dex for both studies), the $[\text{Fe}/\text{H}]$ we measure for MS stars is substantially lower than the figure obtained by Mucciarelli et al. (2011, hereafter M11) for TO stars ($[\text{Fe}/\text{H}] = -1.08$). This is likely due to the different assumptions made about the stellar micro-turbulent velocities. The possible variation of the iron content with the evolutionary stage will be analyzed in a forthcoming contribution (Villanova et al., in preparation). Na abundances were determined from the EWs of the NaD lines at 5889.9 Å and 5895.9 Å and applying the corrections tabulated by Gratton et al. (1999) for non-LTE (NLTE) effects. We have also asked S. Andrievsky and S. Korotin to perform some test computations using their sodium model atom (Korotin & Mishenina, 1999) and version of the multi code (Korotin & Mishenina, 1999), as done in Andrievsky et al. (2007). Their computed NLTE corrections are very similar to those we computed interpolating in the table of Gratton et al. (1999).

We derived stellar lithium abundances from the equivalent width (EW) of the Li I resonance doublet at 6708 Å using the Sbordone et al. (2010) formula B.1³, which takes into account 3D (CO5BOLD) and NLTE effects⁴. We remark that the exact value adopted for the stellar surface gravity, ξ , and iron abundance have minimal impact on the derived Li abundances, which are, instead dominated by the uncertainty in the adopted T_{eff} and in the measured EWs. We estimated the uncertainty for the latter according to the Cayrel formula (Cayrel, 1988) to be 2-3 mÅ, corresponding to 0.06-0.09 dex (Bonifacio et al., 2007). Adding in quadrature to the error implied by a variation of $\Delta T_{\text{eff}} = \pm 150$ K, i.e. an additional 0.09 dex, we end up with a total uncertainty on the Li determination of the order of 0.11-0.13 dex, which we round up to a conservative 0.15 dex. We adopt the same error estimate for Fe and Na abundances as well.

The upper panel of Fig.2 presents the derived Li abundances as a function of the stellar T_{eff} . The Li content is relatively constant at the hottest temperatures and decreases with the temperature for SGB stars. The observed trend and mean abundances are compatible, within the quoted errors, to the M11 results. For stars having $T_{\text{eff}} > 5880$ K, and excluding # 37934 (70 stars), we derive a mean lithium abundance of $\langle A(\text{Li}) \rangle = 2.13 \pm 0.09$ dex (Gaussian dispersion). No correlation of the lithium abundance

³ IDL routines implementing the fitting formulas are available at: <http://mygepi.obspm.fr/~sbordone/fitting.html>

⁴ We computed ad-hoc 3D-NLTE line profile for star # 37934, whose EW is in the extrapolation regime of the formula. We found negligible differences (0.003 dex) with respect to the value computed with formula B.1.

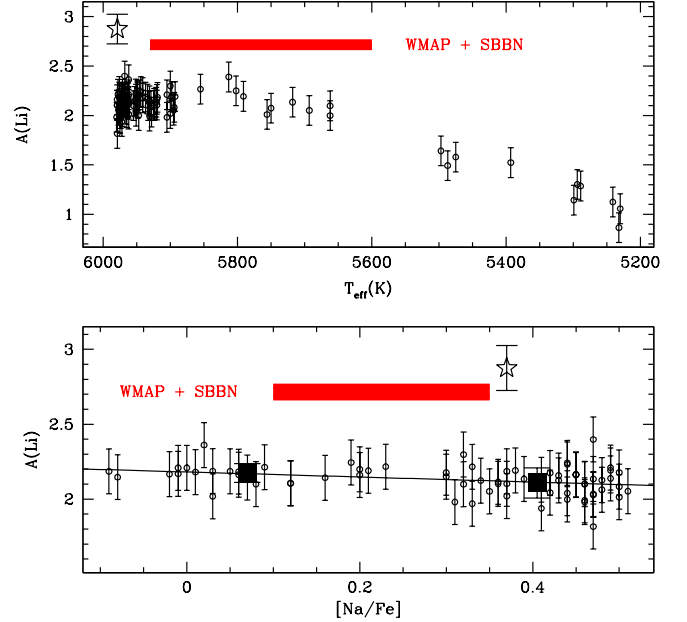


Fig. 2. Measured lithium abundances for targets on the main sequence/sub-giant branch as a function of the effective temperature (upper panel) and the sodium content (lower panel, stars at $T_{\text{eff}} > 5880$ K only). The primordial lithium level implied by WMAP measures plus SBBN theory (shaded area) is also marked for reference. In the lower panel, filled squares indicate the mean Li content for the Na-rich/Na-poor sub-samples. The continuous line is a least square fit to the individual data. In both panels, the big open star marks the position of star # 37934.

with temperature is present among the stars of this sub-sample. M11 derived $\langle A(\text{Li}) \rangle = 2.30 \pm 0.10$ dex for the 35 TO stars in their sample having $T_{\text{eff}} > 5900$ K. The two values are compatible with each other, particularly considering the different T_{eff} scales adopted, the spectral SNR, and the different CMD regions sampled. The iron content has an impact on the Li abundances derived through formula B.1. However, an increase of $\Delta [\text{Fe}/\text{H}] = +0.25$ dex would correspond to a negligible decrease of the lithium abundance of $\Delta A(\text{Li}) = -0.003$ dex.

4. Discussion

Our main results are summarized in the lower panel of Fig.2, where we restrict our analysis to MS stars only ($T_{\text{eff}} > 5880$ K, 71 stars). The cluster stars display a very mild Li-Na anti-correlation. Compared to NGC 6752, in which a spread of 0.6 dex in $[\text{Na}/\text{Fe}]$ corresponds to a spread of 0.6 dex in $A(\text{Li})$ (Pasquini et al., 2005), the anti-correlation in M4 is hardly detectable, with a spread of 0.1 dex in $A(\text{Li})$ corresponding to a spread of 0.6 dex in $A(\text{Na})$. The sample has, however, a Spearman rank correlation coefficient of $C_S = -0.34$, corresponding to a probability of 0.002 that the observed correlation is, in fact, spurious. This conclusion is also supported by an additional non-parametric test (Kendall's tau), as well as by parametric ones. We consider the results of the non-parametric tests as more robust since parametric tests hinge on the correctness of the underlying model – the assumed functional relationship between the variables. On request of the referee, we nevertheless also provide the outcome of the parametric tests (see appendix).

Notice, however, that we detected a very shallow slope and the conclusion we draw below are thus equally applicable to the case of a non detection of a Na-Li anti-correlation.

It would be tempting to interpret the detected anti-correlation by a simple pollution scenario, by which varying quantities of Na-rich/Li-poor material are mixed with “pristine” material. In the case of NGC 6752, it was already pointed out by Shen et al. (2010), however, that such a scenario would imply a slope of one in the A(Li)-A(O) correlation. The fact that the observed slope is significantly different from unity implies that the material is not totally depleted in Li, requiring a production of some Li along with Na. In the same vein, we may argue that the fact that clusters like NGC 6752 and M 4 show similar Na-O anti-correlations (Marino et al., 2008) but different Li-Na anti-correlations, suggests that these anti-correlations arise from the operation of different nuclear reactions which take place at different places, and possibly at different times. If Li were simply destroyed along with Na production, we should always find the same slope of the Li-Na anti-correlation. On the contrary, we need to postulate that Li is produced with different efficiency in different clusters, to explain the absence of a slope in NGC 6397 (Lind et al., 2009), the mild slope in M 4 and the marked slope in NGC 6752. Notice also that the observed slopes do not change in direct correlation with the cluster metallicities. Indeed, D’Orazi & Marino (2010a, hereafter D10) and M11 reached similar conclusions based on the non-detection of a Li-Na/Li-O anti-correlation/correlation among a sample of RGB/TO stars. The two groups of Na-poor/Na-rich stars (arbitrarily separated at $[Na/Fe]=0.25$) have different dispersion around the mean of 0.06 and 0.10, respectively, to be compared with the 0.06 and 0.14 reported by D10.

D’Ercole et al. (2010) presented a class of models capable of reproducing the Na-O and Mg-Al anti-correlations, using AGB stars of the first generation as “polluters”. In their model for M 4, lithium is produced in parallel to the sodium production. These models are quite successful, but depend on several parameters and thus have the possibility of producing the different correlations found in the different clusters. A necessary and key ingredient is the dilution with pristine gas (D’Ercole et al., 2011). A different class of models, in which the “polluters” are fast rotating massive stars (FRMS) has been presented by Decressin et al. (2007, 2010). In this case there is no lithium production and lithium is purely destroyed in the massive stars. The observed lithium is the result of dilution of Li-free matter with pristine material. In a case like that of M 4 the material must clearly be almost pristine, otherwise the variation in Li would be much larger. The observations of the simultaneous, significant variation in the Na content might pose a problem to the viability of such models for M 4. Notice, however, that the recent results by Villanova & Geisler (2011) support FRMS as likely polluters from which the second generation of stars formed in M 4 (see also Yong et al., 2008; Lind et al., 2011).

Figure 2 shows another remarkable fact: there is one star, #37934, that displays a lithium abundance which is significantly higher than that of the others. This star has in fact a lithium content which is compatible with the primordial lithium abundance, as derived from the baryonic density deduced from the fluctuations of the Cosmic Microwave Background and Standard Big Bang Nucleosynthesis (Cyburt et al., 2008, shaded area in Fig.2). The strong Li line of this star can also be appreciated in Figure 1. We have checked individual frames and the strong Li line is detected in all of them. Observations were conducted over a long period, which implies observations with different plates and at different geocentric velocities. Hence, different fibers were used and the star spectrum moved on the CCD. This guaran-

tees that the detection is not spurious. It is natural to pose the question whether it is a case of preservation or production. It is currently accepted that the constant Li abundance displayed by warm metal-poor stars, the so-called *Spite plateau* (Spite & Spite, 1982), falls short by a factor of three to five of the primordial lithium abundance (see Sbordone et al., 2010, and references therein). With the exception of star #37934, the picture we are facing in M 4 is in fact similar to what we see among field stars (the mild Li-Na anti-correlation is hardly significant in this context, see also M11 and Monaco et al., 2010). Notice that the Robin et al. (2003) model predicts no Galactic stars over a one square degree area in the M 4 line of sight with color, magnitude, radial velocity and metallicity similar to #37934, within ± 0.1 mag, ± 0.5 mag, $\pm 3\sigma$ and ± 0.5 dex, in each variable, respectively.

Two metal-poor dwarf stars that lie significantly above the Spite plateau are known, BD +23° 3912 (Bonifacio & Molaro, 1997) and HD 106038 (Asplund et al., 2006). These stars have lithium abundance differences with respect to the cosmological value similar as #37934, but at abundances lower than the cosmological value ($A(Li)=2.72$). The 1D-NLTE lithium abundances of the three stars are $A(Li)=2.83$, 2.59 and 2.48 for #37934, BD +23° 3912 and HD 106038, respectively. Notice that adopting the recent temperature calibrations by González Hernández & Bonifacio (2009), we obtain a temperature 116 K hotter for star #37934 and a corresponding 1D-NLTE abundance of $A(Li)=2.92$. Stars in this metallicity range could already start to feel the effect of the Galactic enrichment in lithium (Romano et al., 1999, 2003). The remarkable difference between star #37934 and BD +23 3912 or HD 106038, is the gap in Li abundance with respect to the reference population: it is ~ 0.7 dex for star #37934 but only ~ 0.3 dex for the other two stars. HD 106038 displays other chemical peculiarities, such as overabundance of Be (Smiljanic et al., 2008), Si, Ni, Y and Ba. Smiljanic et al. (2008) invoke a hypernova to explain such peculiarities, without however, explaining how a star may form from the undiluted hypernova ejecta. It is clear that such an exotic explanation is not applicable to the case of Globular Cluster stars, since the hypernova explosion would expel all gas from the Cluster, thus stopping star-formation.

Also in NGC 6752 and 47 Tuc (Shen et al., 2010; D’Orazi et al., 2010b) there is one star, which, within errors, has a Li abundance compatible with the primordial abundance. In those cases, however, the star lies along a well defined Li-O correlation so that there is a continuity of Li abundances from the highest to the lowest. Here the situation is totally different, as there is no star with a Li content within a factor of 3 of that of #37934.

The nature of this star can be interpreted in different ways. It is currently a matter of debate whether the Spite Plateau originate from a depletion mechanism which is experienced by the stars in a uniform way. Star #37934 might have escaped this depletion which, instead, experienced all the other stars we sampled. In this case the high Li abundance of #37934 would represent a case of preservation of the primordial Li abundance. On the other hand, this star might have followed the same fate of the other stars but might have been created with a higher Li abundance. Its high lithium content would then constitute a case of pollution.

We believe it is hard to rule out any of the two interpretations. In the first case we should identify a mechanism which uniformly depletes lithium in all the cluster stars and another mechanism which suppresses this depletion for star #37934. In the second case, although it is relatively easy to envisage Li production mechanisms, it is not so easy to imagine mechanisms

which would allow this single star to be so much more lithium-rich than the others. The small slope of the Li-Na anti-correlation supports Li production taking place in parallel to Na production. Together with the fact that star #37934 is Na rich (and thus a “second generation star”), this provides circumstantial evidence that favors the second scenario. Additionally, the measures on the single exposures suggest a possible small radial velocity variation at the level of $\sim 1.5 \text{ km s}^{-1}$ over a period of ~ 75 days, which, in turn, may support the pollution scenario from a (now evolved) companion AGB star. An extremely Li-rich giant star has been detected in the Globular Cluster M3 (Kraft et al., 1999). Such Li-rich phases are of short duration, however if the star has an unevolved companion, and transfers Li-rich material onto its atmosphere during this phase, the companion may preserve this Li-rich material. That a local production of Li should result in a lithium abundance matching the primordial lithium abundance would, however, be a remarkable coincidence. Recently, Koch et al. (2011) have reported the detection of a Li-rich dwarf ($A(\text{Li})=4.03$) in the globular cluster NGC 6397. This certainly constitute a case of pollution and reinforces the pollution scenario also for star #37934.

Whichever its origin, star #37934 shows that old, metal-poor, un-evolved stars with the cosmic lithium abundance do exist. We may expect to find other examples of such Li-rich stars in M4 and other clusters. To the extent that a part of the Halo field population may have been formed from stars lost by GCs, we should be able to find similar stars also in the field population.

Acknowledgements. We are grateful to S. Andrievsky and S. Korotin for performing some test NLTE computations for Na. PB acknowledges support from CNRS INSU through PNPS and PNCG grants.

References

- Alonso, A., Arribas, S., & Martínez-Roger, C. 1996, *A&A*, 313, 873
 Andrievsky, S. M., Spite, M., Korotin, S. A., et al. 2007, *A&A*, 464, 1081
 Asplund, M., Lambert, D. L., Nissen, P. E., Primas, F., & Smith, V. V. 2006, *ApJ*, 644, 229
 Bonifacio, P., & Molaro, P. 1997, *MNRAS*, 285, 847
 Bonifacio, P., et al. 2007, *A&A*, 462, 851
 Cayrel, R. 1988, *The Impact of Very High S/N Spectroscopy on Stellar Physics*, 132, 345
 Cannon, R. D., Croke, B. F. W., Bell, R. A., Hesser, J. E., & Stathakis, R. A. 1998, *MNRAS*, 298, 601
 Carretta, E., Bragaglia, A., Gratton, R., D’Orazi, V., & Lucatello, S. 2009, *A&A*, 508, 695
 Cohen, J. G. 1978, *ApJ*, 223, 487
 Cyburt, R. H., Fields, B. D., & Olive, K. A. 2008, *Journal of Cosmology and Astro-Particle Physics*, 11, 12
 Decressin, T., Baumgardt, H., Charbonnel, C., & Kroupa, P. 2010, *A&A*, 516, A73
 Decressin, T., Charbonnel, C., & Meynet, G. 2007, *A&A*, 475, 859
 D’Ercole, A., D’Antona, F., & Vesperini, E. 2011, *MNRAS*, 376
 D’Ercole, A., D’Antona, F., Ventura, P., Vesperini, E., & McMillan, S. L. W. 2010, *MNRAS*, 407, 854
 D’Orazi, V., & Marino, A. F. 2010b, *ApJ*, 716, L166 (D10)
 D’Orazi, V., Lucatello, S., Gratton, R., Bragaglia, A., Carretta, E., Shen, Z., & Zaggia, S. 2010a, *ApJ*, 713, L1
 González Hernández, J. I., & Bonifacio, P. 2009, *A&A*, 497, 497
 Gratton, R. G., Carretta, E., Eriksson, K., & Gustafsson, B. 1999, *A&A*, 350, 955
 Gratton, R. G., et al. 2001, *A&A*, 369, 87
 Harris, W. E. 1996, *AJ*, 112, 1487
 Hesser, J. E. 1978, *ApJ*, 223, L117
 Koch, A., Lind, K., & Rich, R. M. 2011, *ApJ*, 738, L29
 Korotin, S. A., Andrievsky, S. M., & Luck, R. E. 1999, *A&A*, 351, 168
 Korotin, S. A., & Mishenina, T. V. 1999, *Astronomy Reports*, 43, 533
 Korotin, S. A., Andrievsky, S. M., & Kostynchuk, L. Y. 1998, *Ap&SS*, 260, 531
 Korotin, S. A., Andrievsky, S. M., & Kostynchuk, L. Y. 1999, *A&A*, 342, 756
 Kraft, R. P., Peterson, R. C., Guhathakurta, P., Sneden, C., Fulbright, J. P., & Langer, G. E. 1999, *ApJ*, 518, L53
 Kurucz, R. L. 2005, *Memorie della Società Astronomica Italiana Supplementi*, 8, 14
 Iocco, F., Mangano, G., Miele, G., Pisanti, O., & Serpico, P. D. 2009, *Phys. Rep.*, 472, 1
 Ivans, I. I., Sneden, C., Kraft, R. P., Suntzeff, N. B., Smith, V. V., Langer, G. E., & Fulbright, J. P. 1999, *AJ*, 118, 1273
 Lind, K., Primas, F., Charbonnel, C., Grundahl, F., & Asplund, M. 2009, *A&A*, 503, 545
 Lind, K., Charbonnel, C., Decressin, T., Primas, F., Grundahl, F., & Asplund, M. 2011, *A&A*, 527, 148
 Lovisi, L., et al. 2010, *ApJ*, 719, L121
 Marino, A. F., Villanova, S., Piotto, G., Milone, A. P., Momany, Y., Bedin, L. R., & Medling, A. M. 2008, *A&A*, 490, 625
 Momany, Y., Cassisi, S., Piotto, G., Bedin, L. R., Ortolani, S., Castelli, F., & Recio-Blanco, A. 2003, *A&A*, 407, 303
 Monaco, L., Bonifacio, P., Sbordone, L., Villanova, S., & Pancino, E. 2010, *A&A*, 519, L3
 Mucciarelli, A., Salaris, M., Lovisi, L., Ferraro, F. R., Lanzoni, B., Lucatello, S., & Gratton, R. G. 2011, *MNRAS*, 412, 81 (M11)
 Norris, J. 1981, *ApJ*, 248, 177
 Norris, J., & Freeman, K. C. 1983, *ApJ*, 266, 130
 Pasquini, L., Avila, G., Blecha, A., et al. 2002, *The Messenger*, 110, 1
 Pasquini, L., Bonifacio, P., Molaro, P., Francois, P., Spite, F., Gratton, R. G., Carretta, E., & Wolff, B. 2005, *A&A*, 441, 549
 Piotto, G. 2008, *Mem. Soc. Astron. Italiana*, 79, 334
 Robin, A. C., Reylé, C., Derrière, S., & Picaud, S. 2003, *A&A*, 409, 523
 Romano, D., Matteucci, F., Molaro, P., & Bonifacio, P. 1999, *A&A*, 352, 117
 Romano, D., Tosi, M., Matteucci, F., & Chiappini, C. 2003, *MNRAS*, 346, 295
 Sarajedini, A., et al. 2007, *AJ*, 133, 1658
 Sbordone, L., Bonifacio, P., Castelli, F., & Kurucz, R. L. 2004, *Memorie della Società Astronomica Italiana Supplementi*, 5, 93
 Sbordone, L. 2005, *Memorie della Società Astronomica Italiana Supplementi*, 8, 61
 Sbordone, L., et al. 2010, *A&A*, 522, A26
 Shen, Z.-X., Bonifacio, P., Pasquini, L., & Zaggia, S. 2010, *A&A*, 524, L2
 Smiljanic, R., Pasquini, L., Primas, F., Mazzali, P. A., Galli, D., & Valle, G. 2008, *MNRAS*, 385, L93
 Sneden, C. 1973, *ApJ*, 184, 839
 Spite, F., & Spite, M. 1982, *A&A*, 115, 357
 Valcarce, A. A. R., & Catelan, M. 2011, *arXiv:1106.6082*
 Ventura, P., & D’Antona, F. 2010, *MNRAS*, 402, L72
 Villanova, S., et al. 2007, *ApJ*, 663, 296
 Villanova, S., & Geisler, D. 2011, *A&A*, 535, 31
 Yong, D., Lambert, D., Paulson, D.B., Carney, B.W. 2008, *ApJ*, 673, 854

Appendix A: The Na-Li anticorrelation

On request of the referee we provide the results of our parametric tests in this section. The familiar methodology underlying linear regression makes it appealing, however, the reader should be aware that we base our conclusions about the reality of the anti-correlation on the non-parametric tests.

We select only stars with $T_{\text{eff}} > 5880$ and $A(\text{Li}) < 2.6$ thus excluding star #37934 (inclusion of the star does not change the results in any significant way). We perform a straight line fit taking into account errors in both x and y using routine `fitexy` (Press et al., 1992).

We assumed a conservative error of 0.15 dex for the abundances measured in this contribution. 0.15 dex is an appropriate “external” error, however in the context of the Na-Li slope what is relevant is the “internal” error, that is certainly smaller. We assumed an error of 0.09 dex, guided by the R.M.S of the linear fits we performed. Incidentally, this is consistent with the estimated Li abundance variation due to uncertainty in the EW measures.

If we use the LTE Na abundance the slope is -0.30 ± 0.09 corresponding to a 3.3σ detection, the $\chi^2 = 647$ corresponding to a probability of the fit of 0.59. The root mean square deviation around the fitted line is 0.09 dex. Using NLTE Na the slope is -0.22 ± 0.07 corresponding to a 3.1σ detection. The $\chi^2 = 661$ corresponding to a probability of 0.54 and the root mean square deviation around the fitted line is still 0.09 dex.

In summary, the parametric fits fully support the conclusion of the non-parametric tests, suggesting that an anti-correlation between Na and Li exists. Statistical considerations of the goodness-of-fit suggest that the “internal” errors on the abundances are rather of the order of 0.09 dex, while 0.15 dex is a good estimate of the “external” errors.

References

Press, W. H., Teukolsky, S. A., Vetterling, W. T., & Flannery, B. P. 1992, *Numerical Recipes*, Cambridge: University Press, —c1992, 2nd ed.,

Table A.1. Basic data for MS/SGB stars studied in this paper.

ID	RA	Dec	$T_{\text{eff}}(\text{K})$	$\log g$	ξ (kms^{-1})	A(Fe)	A(Na)	A(Li)	EW (mÅ)	S/N
506	16:24:13.10	-26:23:34.70	5933	4.00	1.72	6.16	5.30	2.10	34	87
1024	16:24:12.60	-26:22:28.50	5924	3.99	1.71	6.19	5.37	2.10	34	72
7746	16:23:29.61	-26:24:09.10	5905	3.96	1.71	6.19	5.50	2.21	44	125
8029	16:23:48.66	-26:23:35.10	5921	3.98	1.71	6.18	5.39	2.13	37	121
8332	16:23:47.95	-26:22:50.00	5928	3.99	1.72	6.17	5.46	2.03	30	107
8405	16:23:39.36	-26:22:40.20	5900	3.95	1.71	6.17	5.31	2.30	52	121
8784	16:23:36.47	-26:21:40.20	5951	4.02	1.72	6.18	4.98	2.17	38	104
9139	16:23:49.05	-26:20:40.90	5905	3.95	1.71	6.13	5.41	1.98	28	110
9254	16:23:41.92	-26:20:18.90	5475	3.69	1.06	6.28	5.44	1.58	25	139
9280	16:23:44.05	-26:20:13.10	5976	4.10	1.73	6.21	4.94	2.18	38	95
9505	16:23:48.90	-26:19:26.80	5920	3.97	1.71	6.21	5.15	2.11	35	96
13512	16:23:05.69	-26:22:49.70	5967	4.06	1.72	6.17	5.46	2.13	35	94
13810	16:23:03.38	-26:21:58.30	5947	4.01	1.72	6.17	5.43	2.00	27	88
28521	16:23:13.71	-26:38:57.30	5963	4.05	1.72	6.20	5.32	2.18	38	89
28814	16:23:11.56	-26:38:13.70	5898	3.95	1.71	6.19	5.50	2.19	43	113
30253	16:23:13.10	-26:35:02.60	5230	3.48	1.04	6.36	5.51	1.06	13	131
30699	16:23:15.92	-26:34:06.30	5791	3.86	1.69	6.19	5.06	2.19	50	152
30887	16:23:15.82	-26:33:42.40	5931	3.99	1.72	6.23	5.35	2.15	38	127
31190	16:23:14.43	-26:33:06.90	5971	4.07	1.72	6.14	5.40	2.04	28	73
31634	16:23:12.07	-26:32:15.20	5241	3.50	1.04	6.34	5.28	1.12	15	120
31931	16:23:12.77	-26:31:44.60	5299	3.57	1.04	6.34	5.50	1.14	14	148
32111	16:23:13.32	-26:31:25.10	5974	4.08	1.72	6.18	5.37	2.10	32	126
32349	16:23:11.46	-26:31:00.60	5294	3.57	1.04	6.31	5.32	1.30	19	144
32890	16:23:15.02	-26:30:01.90	5693	3.79	1.55	6.23	5.16	2.05	44	138
32992	16:23:13.75	-26:29:50.10	5975	4.08	1.72	6.19	5.43	2.17	37	89
33132	16:23:10.36	-26:29:30.70	5979	4.13	1.73	6.17	5.19	2.16	36	99
33215	16:23:15.08	-26:29:20.00	5979	4.10	1.73	6.14	5.42	2.10	32	101
33303	16:23:08.57	-26:29:08.30	5750	3.83	1.68	6.19	5.45	2.07	43	128
33349	16:22:50.71	-26:29:02.80	5975	4.09	1.72	6.21	5.36	1.97	24	83
33462	16:23:16.48	-26:28:49.20	5662	3.77	1.48	6.22	5.10	2.10	51	102
33518	16:23:13.79	-26:28:42.30	5497	3.70	1.11	6.29	5.37	1.64	27	151
33548	16:23:07.86	-26:28:38.00	5289	3.57	1.04	6.29	5.12	1.29	19	123
33744	16:23:13.91	-26:28:13.30	5894	3.95	1.71	6.16	5.48	2.08	35	129
33789	16:23:15.40	-26:28:08.00	5813	3.87	1.69	6.17	5.11	2.39	69	140
33879	16:23:10.13	-26:27:55.90	5977	4.09	1.73	6.20	5.37	2.05	29	100
34383	16:22:49.09	-26:26:46.00	5962	4.05	1.72	6.21	5.05	2.36	54	106
35614	16:23:28.79	-26:40:27.10	5953	4.03	1.72	6.22	5.11	2.14	36	110
35854	16:23:40.92	-26:40:12.10	5969	4.06	1.72	6.18	5.03	2.19	38	105
36554	16:23:40.47	-26:39:19.70	5919	3.97	1.71	6.18	5.06	2.18	41	119
36853	16:23:37.06	-26:38:58.60	5964	4.05	1.72	6.20	5.23	2.19	39	81
36867	16:23:19.42	-26:38:57.90	5920	3.98	1.71	6.26	5.14	2.16	39	103
37028	16:23:25.09	-26:38:45.80	5893	3.94	1.71	6.21	5.41	2.19	43	119
37156	16:23:27.21	-26:38:38.40	5931	3.99	1.72	6.24	5.52	1.99	27	114
37166	16:23:35.88	-26:38:37.90	5393	3.65	1.03	6.35	5.36	1.52	26	141
37222	16:23:20.13	-26:38:34.60	5895	3.95	1.71	6.16	5.49	2.05	33	111
37934	16:23:23.71	-26:37:42.30	5979	4.11	1.73	6.16	5.35	2.87	114	75
38327	16:23:30.82	-26:37:15.90	5941	4.01	1.72	6.18	5.44	2.23	44	109
38391	16:23:45.59	-26:37:11.20	5978	4.10	1.73	6.25	5.16	2.21	40	96
38464	16:23:36.34	-26:37:06.20	5949	4.02	1.72	6.13	5.32	2.19	39	117
38485	16:23:46.46	-26:37:04.30	5951	4.02	1.72	6.13	5.37	2.04	29	101
38547	16:23:28.74	-26:37:00.10	5924	3.98	1.71	6.23	5.39	2.12	36	112
38548	16:23:27.21	-26:37:00.10	5487	3.69	1.09	6.34	5.47	1.49	20	117
38573	16:23:22.03	-26:36:57.80	5968	4.06	1.72	6.16	5.45	2.40	57	98
38597	16:23:40.83	-26:36:56.10	5934	4.00	1.72	6.17	5.44	2.17	39	109
39344	16:23:24.33	-26:36:15.30	5962	4.04	1.72	6.19	5.51	2.01	27	95
39639	16:23:23.37	-26:36:02.20	5955	4.03	1.72	6.12	5.40	2.10	33	109
39862	16:23:21.73	-26:35:52.80	5662	3.77	1.48	6.24	5.43	2.00	42	138
43701	16:23:46.92	-26:33:20.40	5969	4.06	1.72	6.16	5.43	2.16	36	126
56218	16:23:25.02	-26:27:19.70	5718	3.81	1.61	6.20	5.29	2.13	50	126
57062	16:23:46.57	-26:26:54.80	5962	4.04	1.72	6.16	5.14	2.14	35	103
57261	16:23:23.78	-26:26:48.90	5232	3.49	1.04	6.35	5.51	0.86	8	115
57631	16:23:24.06	-26:26:37.30	5756	3.83	1.68	6.25	5.52	2.01	37	122
57794	16:23:27.07	-26:26:32.20	5979	4.11	1.73	6.17	5.11	2.11	32	104
58082	16:23:22.16	-26:26:22.40	5949	4.02	1.72	6.21	5.23	2.20	40	114
58089	16:23:20.59	-26:26:22.20	5972	4.07	1.72	6.24	4.98	2.15	35	104

Table A.1. continued.

ID	RA	Dec	T _{eff} (K)	log g	ξ (kms ⁻¹)	A(Fe)	A(Na)	A(Li)	EW (mÅ)	S/N
58440	16:23:43.05	-26:26:10.50	5979	4.11	1.73	6.18	5.47	1.82	18	107
58482	16:23:35.34	-26:26:09.10	5968	4.06	1.72	6.23	5.48	2.12	34	125
58580	16:23:47.24	-26:26:05.80	5965	4.06	1.72	6.19	5.48	2.03	28	105
58671	16:23:30.37	-26:26:03.00	5980	4.11	1.73	6.22	5.35	1.98	25	120
58759	16:23:42.47	-26:25:59.70	5855	3.91	1.70	6.21	5.34	2.27	52	142
59664	16:23:49.67	-26:25:26.60	5967	4.07	1.72	6.20	5.01	2.17	37	112
60462	16:23:23.79	-26:24:54.80	5973	4.07	1.72	6.18	5.01	2.18	38	95
60508	16:23:21.25	-26:24:53.00	5946	4.01	1.72	6.25	5.06	2.21	41	119
60599	16:23:22.44	-26:24:49.40	5976	4.09	1.72	6.26	5.27	2.24	43	119
63647	16:24:07.51	-26:35:36.50	5964	4.05	1.72	6.17	5.48	2.14	35	91
63900	16:23:59.44	-26:35:06.00	5966	4.06	1.72	6.19	5.49	2.06	30	89
64263	16:24:05.88	-26:34:24.20	5951	4.02	1.72	6.17	5.22	2.22	42	96
65049	16:24:09.05	-26:32:56.80	5972	4.08	1.72	6.16	5.41	2.16	36	89
65318	16:24:01.82	-26:32:24.60	5937	4.00	1.72	6.16	5.03	2.19	40	107
65824	16:24:11.26	-26:31:28.80	5802	3.87	1.69	6.17	5.29	2.25	55	113
65935	16:24:03.79	-26:31:17.50	5963	4.05	1.72	6.17	5.40	2.13	34	135
65939	16:24:21.11	-26:31:17.30	5900	3.95	1.71	6.14	4.99	2.02	30	103
66076	16:24:08.33	-26:31:02.10	5941	4.01	1.72	6.14	5.46	2.18	39	115
66136	16:24:09.44	-26:30:55.80	5944	4.01	1.72	6.19	5.45	2.24	44	118
66304	16:24:20.05	-26:30:36.50	5974	4.08	1.72	6.17	5.36	2.02	27	91
66558	16:24:09.93	-26:30:08.90	5962	4.05	1.72	6.26	5.44	2.11	34	106
66764	16:24:17.72	-26:29:47.10	5971	4.08	1.72	6.25	5.40	2.22	41	106
67406	16:24:17.26	-26:28:36.00	5949	4.02	1.72	6.15	5.45	2.13	35	128
67707	16:24:20.28	-26:28:03.30	5972	4.07	1.72	6.14	5.37	1.94	23	83
67796	16:24:22.25	-26:27:51.60	5929	3.99	1.72	6.19	5.09	2.10	34	94
68022	16:24:19.37	-26:27:24.40	5962	4.04	1.72	6.17	4.99	2.21	40	97

Notes. For each star, we report ID, J2000 equatorial coordinates, atmospheric parameters, the Fe, Na and Li abundances, the Li line EWs and the spectral S/N at the lithium line.